

## Radially dependent antishielding factor $\gamma(r)$ of the $\text{Sc}^{3+}$ ion in the solid state

B B PANIGRAHI, N C MOHAPATRA<sup>1</sup> and S HAFIZUDDIN<sup>2</sup>

Department of Physics, Khallikote (Autonomous) College, Berhampur 760 001, India

<sup>1</sup>Department of Physics, Berhampur Univeristy, Berhampur 760 001, India

<sup>2</sup>Department of Physics, B.J.B. College, Bhubaneswar 751 001, India

MS received 13 November 1996; revised 16 July 1997

**Abstract.** We report the results of our calculation of  $\gamma(r)$ , the radially dependent antishielding factor of  $\text{Sc}^{3+}$  ion in the crytalline environment. Watson sphere model is used to approximately represent the crystal potential. Differential equations resulting from non-orthogonal Hartree–Fock perturbation theory are solved to obtain perturbations to core electron states. Contribution to  $\gamma(r)$  from electron self-consistency effect has been evaluated by using the latter wave-functions in the many-body expression of Schmidt *et al.*

**Keywords.** Radially dependent antishielding factor; crystalline potential; electron-electron self consistency effect.

PACS Nos 32.10; 31.70

### 1. Introduction

It is well known [1–3] that when source charges, such as conduction electrons in metals, are inside the core region of the atoms, antishielding effect of the core states becomes radially dependent. If the perturbation of the core states is by the nuclear quadrupole moment  $Q$ , the antishielding factor is referred [2] to as  $\gamma(r)$ . The latter plays an important role in the calculation of electric field gradient (EFG) in metals. In most of the early calculations [4–6] of EFG in metals,  $\gamma(r)$  has been set equal to zero primarily because the latter quantities were not available at the time of these calculations. In a few cases [7, 8] where  $\gamma(r)$  values were available, these were not used in EFG calculations perhaps for two reasons: First these were obtained for a free ion instead of an ion in solid state. Secondly, the calculated results of  $\gamma(r)$  did not include the so called electron self-consistency contribution which, in general, is not negligible.

With the introduction of Watson sphere model [9], it has now been possible to approximately include the crystalline effect on  $\gamma(r)$ . As to the consistency contribution, it has been shown by Ray *et al* [10] as well as Beri *et al* [11] that the total consistency contribution  $\gamma_{\infty}^{(1)}$  can be evaluated from their many-body expression using the perturbation of the core electron states obtained in differential equation procedures [2, 12]. Following their [10, 11] suggestions, Schmidt *et al* [13] have calculated  $\gamma_{\infty}^{(1)}$  for a large number of positive and negative ions both in free and crystalline states. A further

extension has been subsequently made by Tripathi and Mohapatra [14] for evaluating  $\gamma^{(1)}(r)$ , the radially dependent consistency contribution, from the expression of  $\gamma_{\infty}^{(1)}$  originally due to Ray *et al* [10].

We have followed closely the procedure of Tripathi and Mohapatra [14] for evaluating  $\gamma(r)$  in  $\text{Sc}^{3+}$  ion in solid state. The reasons for taking up Sc are two-fold: First  $\gamma(r)$  for this ion is not available either in free state or in the solid state. Secondly, we wish to use these results in the calculation of EFG in Sc metal to study the change it may produce in the EFG obtained recently [15, 16] with an approximate  $\gamma(r)$ .

We wish to remark here that there are a number of procedures in which EFG can be evaluated without using  $\gamma(r)$  explicitly. These are: (a) linearized augmented plane wave method [17, 18], (b) linear muffin-tin-orbital method [19, 20], (c) augmented spherical wave method [21], (d) linear combination of atomic orbital method [22] and the procedure due to Meyer *et al* [23]. In the latter procedure [23], various schemes are developed to reconstruct the true wave functions from the pseudo wave functions in crystals and EFG is evaluated with good accuracy using the true wave functions.

The paper is organized as follows: In § 2, we briefly describe the theory. Results and discussion are presented in § 3. Section 4 summarizes the conclusions.

## 2. Theory

If consistency contribution is neglected, the resulting antishielding factor, referred to as the zero-order contribution and denoted by  $\gamma^{(0)}(r)$  is given [14] by

$$\gamma^{(0)}(r) = \frac{1}{Q} \left( \int_0^r Q_i^{(0)}(r') dr' + r^5 \int_r^{\infty} Q_i^{(0)}(r') (r')^{-5} dr' \right), \quad (1)$$

where

$$Q_i^{(0)}(r) = Qr^2 \sum_n C_{l_0 l}^{(2)} U'_0(nl, r) V'_1(nl \rightarrow l_0, r). \quad (2)$$

In eq. (2)  $U'_0$  is the radial part of the unperturbed core state.  $V'_1$  is the radial part of the perturbation in the core state and is obtained in the differential equation procedure of non-orthogonal Hartree–Fock perturbation theory (NHFPT) of Dalgarno [24]. Other symbols have their usual meanings. Following the procedure of Tripathi and Mohapatra [14], the radially dependent consistency contribution can similarly be expressed as

$$\gamma^{(1)}(r) = \frac{1}{Q} \left( \int_0^r Q_i^{(1)}(r') dr' + r^5 \int_r^{\infty} Q_i^{(1)}(r') (r')^{-5} dr' \right), \quad (3)$$

where  $Q_i^{(1)}(r)$  is interpreted as the induced quadrupole moment density in the core electrons due to the consistency effect. In obtaining consistency contribution [10], one considers the simultaneous excitation of a pair of electrons. Correspondingly, one may have contributions from radial, angular and mixed modes of excitations. In the radial mode, both the core electrons are excited into states with unchanged  $l$  values. In the angular mode both the core electrons are excited into states with  $l \pm 2$  values. In the mixed mode while one is excited to a state with same  $l$ , the other goes to  $l \pm 2$  state. For convenience, we will refer to the sum of angular and the mixed mode as the ‘angular mode’ contribution.

### Radially dependent antishielding factors

It has been noted by Schmidt *et al* [13] that the contribution to  $\gamma_{\infty}^{(1)}$  from the ‘angular mode’ is quite negligible compared to the radial mode. In the present calculation we have neglected the former.

For  $p$ -core ions, the expressions for  $Q_i^{(1)}(r)$  have been worked out by Tripathi and Mohapatra [14]. These expressions, in addition to depending on  $U'_0, V'_1$  functions also involve  $\bar{V}'_1$ , the radial part of the perturbed core states in EFG-perturbation. For details the reader may refer to the work of Tripathi and Mohapatra [14].

### 3. Results and discussion

Hartree–Fock (HF) wave functions of ions in free state as well as in crystalline state, the latter being evaluated in Watson sphere model [9] are available from the work of Paschalis and Weiss [25]. The core wave functions of  $\text{Sc}^{3+}$  ion in crystalline state corresponding to Pauling [26] ionic radius,  $r_0 = 0.81 \text{ \AA}$ , are used in the present work. These are taken from the work of Paschalis and Weiss [25]. Out of the five core states,  $1s-3p$  of  $\text{Sc}^{3+}$ , the  $s$ -core states contribute to  $\gamma^{(0)}(r)$  through only the angular mode of excitation, the two  $p$ -core states contribute both in radial and angular modes. Out of these  $\gamma_{\text{ang}}^{(0)}(r)$ , the net angular mode contribution to  $\gamma^{(0)}(r)$  is generally small and negligible compared to the more important radial mode contribution,  $\gamma_{\text{rad}}^{(0)}(r)$ , but the former takes more computation time than the latter. For this reason,  $\gamma_{\text{ang}}^{(0)}(r)$  has been evaluated using a modified Thomas–Fermi model for the charge distribution in exactly the same way as it was done in the previous work [12].

The radial mode contribution  $\gamma_{\text{rad}}^{(0)}(r)$ , on the other hand, has been evaluated exactly by using the appropriate HF wave function  $U'_0(2p, r)$  and  $U'_0(3p, r)$  of  $2p$  and  $3p$  core electrons. The differential equations in the perturbations  $V_1(np \rightarrow p, r)$  and  $\bar{V}_1(np \rightarrow p, r)$  are solved using a non-iterative procedure due to Duff and Das [27]. These functions are then orthogonalized to the occupied core states in order to avoid violation of exclusion principle. In the numerical solution of the differential equations in  $V_1$  and  $\bar{V}_1$ , a logarithmic scale with 209 mesh points has been chosen. The  $r$ -value of the  $n$ th mesh point in this scale is obtainable from the relation,  $r_n = Z^{-1} \exp[-3.0 + (n-1)h]$ , where  $Z$  is the atomic number of Sc and  $h = 0.045$ . The largest value of  $r$  in this choice of mesh points is  $r_{209} = 27.536$  atomic units (au).

In figures 1 and 2, we have plotted the orthogonalized solutions  $V'_1$  for the  $2p$  and  $3p$  core states of  $\text{Sc}^{3+}$  ion in solid state. These have the same number of nodes as of a  $4p$  atomic core state in agreement with the expectation from perturbation of  $2p$  and  $3p$  states in the radial modes. In figure 3 the total  $\gamma^{(0)}(r)$ , that is, the sum of  $\gamma_{\text{rad}}^{(0)}(r)$  and  $\gamma_{\text{ang}}^{(0)}(r)$  is plotted as a function of  $r$ . The nature of its variation with  $r$  leading to a nearly constant value at large  $r$  is as expected.

The consistency contribution  $\gamma^{(1)}(r)$ , has been evaluated using the expressions derived in the work of Tripathi and Mohapatra [14]. In doing so the contributions from the radial mode have been calculated exactly. On the other hand, the contribution from the ‘angular mode’ which is generally smaller than the radial mode, but takes more computation time has been neglected in the present work. The error due to this neglect is negligible. It may be noted here that unlike  $\text{Na}^+$  ion [14], which has only  $2p$  core electrons,  $\text{Sc}^{3+}$  ions has both  $2p$  and  $3p$  core electrons. Therefore, in the latter ion, contribution to  $\gamma^{(1)}(r)$

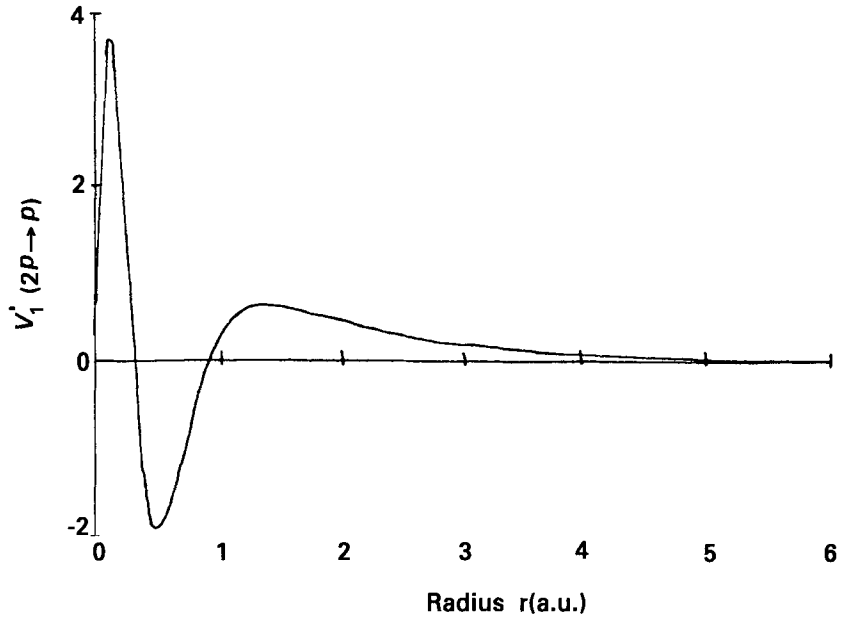


Figure 1. Perturbed function  $V'_1(2p \rightarrow p)$  of  $Sc^{3+}$  ion in solid state.

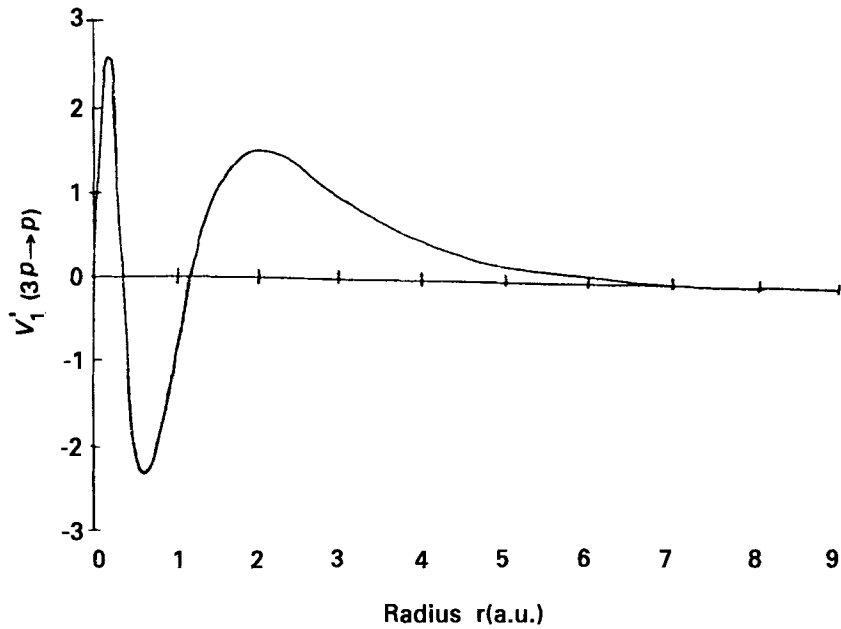
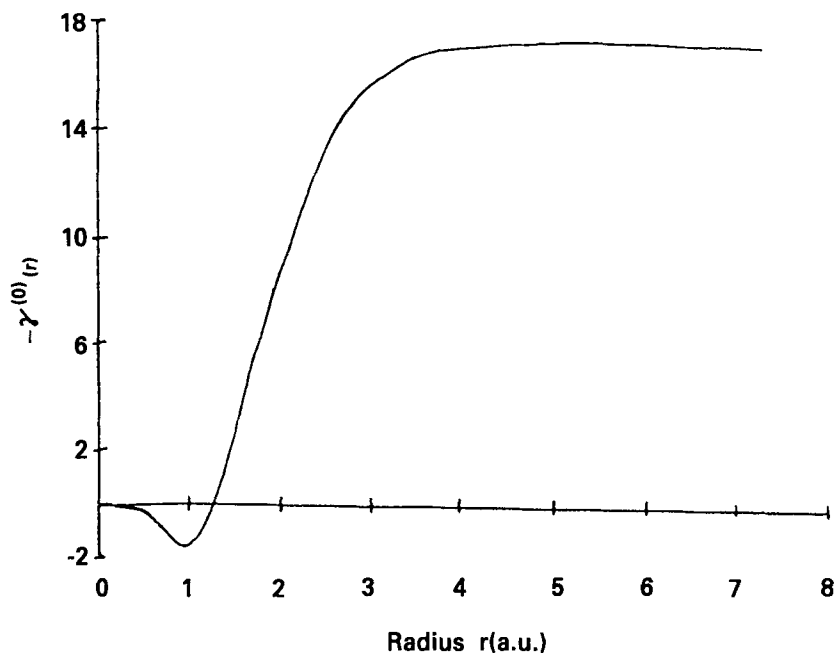


Figure 2. Perturbed function  $V'_1(3p \rightarrow p)$  of  $Sc^{3+}$  ion in solid state.

arises both from intrashell and intershell pair excitations of  $p$ -core electrons. In figure 4  $\gamma^{(1)}(r)$  is plotted. The variation with  $r$  is similar to those observed in case of other ions [14].

*Radially dependent antishielding factors*



**Figure 3.** The radially dependent antishielding factor  $\gamma^{(0)}(r)$  of  $\text{Sc}^{3+}$  ion in solid state.

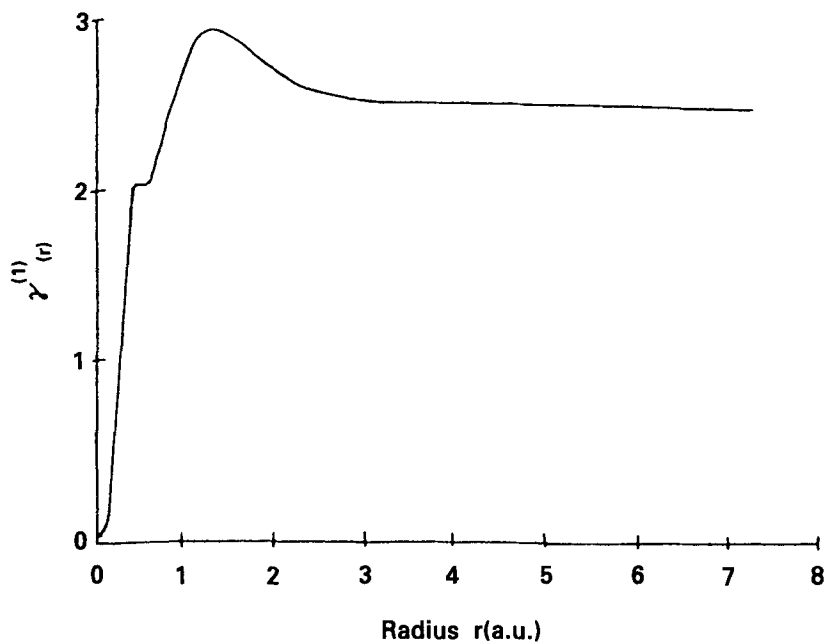


**Figure 4.** Self-consistency contribution  $\gamma^{(1)}(r)$  to radially dependent antishielding factor of  $\text{Sc}^{3+}$  ion in solid state.

**Table 1.** The radially dependent antishielding factors  $\gamma_{\text{rad}}^{(0)}(r)$ ,  $\gamma_{\text{ang}}^{(0)}(r)$ ,  $\gamma^{(0)}(r)$ ,  $\gamma^{(1)}(r)$  and  $\gamma_{\text{tot}}(r)$  of  $\text{Sc}^{3+}$  ion in solid state.  $r$  is expressed in atomic units and  $n$  denotes the index of the mesh points.

$n(r)$	$r$	$\gamma_{\text{rad}}^{(0)}(r)$	$\gamma_{\text{ang}}^{(0)}(r)$	$\gamma^{(0)}(r)$	$\gamma^{(1)}(r)$	$\gamma_{\text{tot}}(r)$
1	0.0024	0.0000	0.0001	0.0001	-0.0000	0.0001
69	0.0505	0.0011	0.0165	0.0176	-0.0501	-0.0325
79	0.0793	0.0067	0.0312	0.0379	-0.2061	-0.1681
85	0.1038	0.0171	0.0456	0.0627	-0.4244	-0.3617
93	0.1488	0.0461	0.0745	0.1206	-0.9288	-0.8082
100	0.2040	0.0725	0.1132	0.1857	-1.5059	-1.3202
105	0.2555	0.0596	0.1516	0.2112	-1.8553	-1.6441
120	0.5018	-0.0997	0.3455	0.2458	-2.0350	-1.7892
124	0.6008	0.1156	0.4232	0.5388	-2.1663	-1.6275
128	0.7193	0.5176	0.5128	1.0304	-2.4176	-1.3872
133	0.9007	0.8775	0.6376	1.5151	-2.7595	-1.2444
136	1.0309	0.6266	0.7177	1.3443	-2.8976	-1.5533
138	1.1280	0.1123	0.7728	0.8851	-2.9437	-2.0586
140	1.2343	-0.7414	0.8287	0.0873	-2.9520	-2.8647
141	1.2911	-1.3018	0.8570	-0.4448	-2.9430	-3.3878
142	1.3505	-1.9535	0.8854	-1.0681	-2.9271	-3.9952
143	1.4127	-2.6871	0.9138	-1.7733	-2.9046	-4.6779
144	1.4777	-3.5029	0.9423	-2.5606	-2.8777	-5.4383
145	1.5457	-4.3829	0.9707	-3.4122	-2.8468	-6.2590
146	1.6168	-5.3261	0.9990	-4.3271	-2.8141	-7.1412
147	1.6913	-6.3089	1.0271	-5.2818	-2.7801	-8.0619
148	1.7691	-7.3307	1.0550	-6.2757	-2.7468	-9.0225
149	1.8505	-8.3639	1.0826	-7.2813	-2.7143	-9.9956
150	1.9357	-9.4063	1.1099	-8.2964	-2.6842	-10.981
151	2.0248	-10.4300	1.1367	-9.2933	-2.6563	-11.950
153	2.2155	-12.386	1.189	-11.197	-2.6099	-13.807
155	2.4241	-14.131	1.239	-12.892	-2.5759	-15.468
156	2.5357	-14.902	1.263	-13.639	-2.5634	-16.203
158	2.7745	-16.202	1.308	-14.894	-2.5453	-17.439
160	3.0358	-17.181	1.350	-15.831	-2.5347	-18.366
163	3.4746	-18.105	1.405	-16.700	-2.5271	-19.227
172	5.2095	-18.775	1.518	-17.257	-2.5243	-19.781
175	5.9624	-18.783	1.539	-17.244	-2.5241	-19.769
179	7.1383	-18.784	1.556	-17.228	-2.5241	-19.752
180	7.4669	-18.784	1.556	-17.228	-2.5241	-19.752
209	27.536	-18.784	1.556	-17.228	-2.5241	-19.752

In addition to these figures, we have also summarized the data in table 1. Instead of listing the values of  $\gamma^{(0)}$  and  $\gamma^{(1)}$  at all the 209 mesh points, we have chosen for the sake of brevity, to list the values at thirty-five representative mesh points, so that the broad features of  $\gamma^{(0)}$  and  $\gamma^{(1)}$  (figures 3 and 4), namely, node/hump in small  $r$  region and near constancy in the large  $r$  region are represented by this smaller set of selected mesh points. The first column gives the  $n$ -value of the mesh point while the second column gives the  $r$  value corresponding to this  $n$ . Columns 3–7 list the contributions  $\gamma_{\text{rad}}^{(0)}(r)$ ,  $\gamma_{\text{ang}}^{(0)}(r)$ ,  $\gamma^{(0)}(r)$ ,  $\gamma^{(1)}(r)$  and  $\gamma_{\text{tot}}(r)$ , the last one being the sum of  $\gamma^{(0)}(r)$  and  $\gamma^{(1)}(r)$ . From this table, the saturation values of  $\gamma^{(0)}$ ,  $\gamma^{(1)}$  and  $\gamma_{\text{tot}}$  are noted to be  $-17.23$ ,  $-2.52$  and  $-19.75$

respectively, which may be regarded as equal to the respective Sternheimer antishielding factor  $\gamma_{\infty}^{(0)}$ ,  $\gamma_{\infty}^{(1)}$  and  $\gamma_{\infty}$  caused by source charges at infinity.

As  $\gamma^{(0)}(r)$  and  $\gamma^{(1)}(r)$  from other works are not available, it is not possible to compare the present results with others. However, the values of  $\gamma_{\infty}^{(0)}$ ,  $\gamma_{\infty}^{(1)}$ , and  $\gamma_{\infty}$  for  $\text{Sc}^{3+}$  ion in solid state are available from the work of Schmidt *et al* [13]. Their values are:  $\gamma_{\infty}^{(0)} = -20.46$ ,  $\gamma_{\infty}^{(1)} = -2.644$  and  $\gamma_{\infty} = -23.104$ . Comparing these values with those in the present work, we find the present results are smaller in magnitude than those of Schmidt *et al* [13]. The discrepancy between the present results and those of Schmidt *et al* [13] may be attributed to the different ionic radii at which the unperturbed core wave functions are evaluated in Watson sphere model [9]. While the HF wave functions used in the work of Schmidt *et al* [13] correspond to  $r_0 = 0.73 \text{ \AA}$ , those in the present work refer to Pauling radius  $r_0 = 0.81 \text{ \AA}$ . In case of positive ions, as can be seen from the work of Schmidt *et al* [13], a larger  $r_0$  gives values for  $\gamma_{\infty}^{(0)}$  and  $\gamma_{\infty}^{(1)}$  with smaller magnitudes. For negative ions, the trend is opposite. In the present work  $r_0 (= 0.81 \text{ \AA})$  being larger than  $0.73 \text{ \AA}$ , the latter value used by Schmidt *et al* [13], the present results of  $\gamma_{\infty}^{(0)}$  and  $\gamma_{\infty}^{(1)}$  are smaller in magnitude than theirs, as expected. We would like to add here that contribution arising from higher order electron correlation effect which is expected to be still smaller than consistency contribution has been neglected in the present work.

Another pertinent point to discuss is the relative magnitudes of  $\gamma^{(0)}(r)$  and  $\gamma^{(1)}(r)$ . Considering the source from which  $\gamma^{(1)}(r)$  results, one expects it to have smaller magnitude than  $\gamma^{(0)}(r)$ . This is borne out by the data in table 1 for  $r$  larger than about 1.6 au. But for  $r < 1.6$  au,  $\gamma^{(1)}(r)$  is found larger in magnitude than  $\gamma^{(0)}(r)$ . In a bid to understand this we have separately listed  $\gamma_{\text{rad}}^{(0)}(r)$  and  $\gamma_{\text{ang}}^{(0)}(r)$  which make up  $\gamma^{(0)}(r)$ . In the small  $r$  region,  $\gamma_{\text{rad}}^{(0)}(r)$  starts from a small positive value, attains a maximum and then decreases and becomes negative.  $\gamma_{\text{ang}}^{(0)}(r)$ , on the other hand, is positive and gradually increases. In contrast,  $\gamma^{(1)}(r)$  is negative and gradually increases in magnitude. This trend is more or less the same as observed in case of  $\text{Na}^+$  ion in the work of Tripathi and Mohapatra [14]. We do not have a simple explanation for this. It may be due to the complicated dependence of  $\gamma^{(1)}(r)$  on the functions  $U'_0$ ,  $V'_1$  and  $\bar{V}'_1$  in the small  $r$  region. As to the neglected 'angular contribution' to  $\gamma^{(1)}(r)$ , we expect it to be much smaller than 1.57, the saturation value of  $\gamma_{\text{ang}}^{(0)}(r)$ . If one assumes that the 'angular contribution' to  $\gamma^{(1)}(r)$  scales down in the same ratio as  $\gamma_{\text{rad}}^{(1)}(r)$  does in relation to  $\gamma_{\text{rad}}^{(0)}(r)$ , the saturation value of  $\gamma_{\text{ang}}^{(1)}(r)$ , the 'angular contribution' will be less than 0.22.

Before we conclude this section we wish to discuss the sensitiveness of  $\gamma(r)$  to the Watson sphere radius. This type of study has been made by Schmidt *et al* [13] in  $\text{Cl}^-$ . In  $\text{Sc}^{3+}$ , as we have stated before, the value of  $\gamma_{\infty}$  changes from  $-19.75$  to  $-23.104$  when the radius  $r_0$  changes from  $0.81 \text{ \AA}$  to  $0.73 \text{ \AA}$ . That is,  $\gamma_{\infty}$  changes by 17% for a change of 10% in  $r_0$ . The change in  $\gamma(r)$  for individual  $r$  may be slightly different from this. The uncertainty in Pauling [26] ionic radius which is used for  $r_0$  in the present work is expected [13] to be less than 10%. This suggests that the change in the present result due to any uncertainty in Pauling ionic radius will be much less than 17%. It is for this reason, we expect that the EFG in Sc metal when calculated by using the present results of  $1 - \gamma(r)$  would not significantly change if the actual ionic radius differs from the Pauling radius ( $0.81 \text{ \AA}$ ) by less than 10%. However, the exact change can be determined if one repeats the calculation of EFG using  $\gamma(r)$  corresponding to the aforesaid two values of  $r_0$ . Such calculations are planned for future.

#### 4. Conclusion

Radially-dependent antishielding factor  $\gamma(r)$  of  $\text{Sc}^{3+}$  ion in crystalline state has been evaluated in the differential equation procedure of non-orthogonal Hartree–Fock perturbation theory. Consistency contribution from the dominant radial mode of excitation has also been included. The present results of  $\gamma(r)$  may be used in the calculation of EFG in Sc metal for obtaining better accuracy than those in other procedures where  $\gamma(r)$  is either neglected or poorly approximated.

#### References

- [1] H M Foley, R M Sternheimer and D Tyoko, *Phys. Rev.* **83**, 734 (1954)
- [2] R M Sternheimer, *Phys. Rev.* **146**, 140 (1966)
- [3] E H Hygh and T P Das, *Phys. Rev.* **143**, 452 (1966)
- [4] N C Mohapatra, C M Singal, T P Das and P Jena, *Phys. Rev. Lett.* **29**, 456 (1972)
- [5] P Jena, S D Mohanti and T P Das, *Phys. Rev.* **B7**, 975 (1973)
- [6] N C Mohapatra, C M Singal and T P Das, *Phys. Rev. Lett.* **31**, 530 (1973)
- [7] S K Padhi and N C Mohapatra, *Phys. Rev.* **B29**, 5199 (1984)
- [8] B K Acharya and N C Mohapatra, *Pramana – J. Phys.* **43**, 391 (1994)
- [9] R E Watson, *Phys. Rev.* **111**, 1108 (1958)
- [10] S N Ray, T Lee, T P Das and R M Sternheimer, *Phys. Rev.* **A9**, 1108 (1974)
- [11] A C Beri, S N Ray, T P Das and R M Sternheimer, *Phys. Rev.* **A12**, 1168 (1975)
- [12] K K Prasad Rao and N C Mohapatra, *Phys. Rev.* **A24**, 10 (1981)
- [13] P C Schmidt, K D Sen, T P Das and Al Weiss, *Phys. Rev.* **B22**, 4167 (1980)
- [14] P Tripathi and N C Mohapatra, *J. Phys.* **B23**, 3241 (1990)
- [15] B B Panigrahi and N C Mohapatra, *Pramana – J. Phys.* **41**, 443 (1993)
- [16] B B Panigrahi and N C Mohapatra, *Pramana – J. Phys.* **43**, 407 (1994)
- [17] D D Koelling and G O Arbman, *J. Phys.* **F5**, 2041 (1975)
- [18] P Blaha, K Schwarz and P H Dederichs, *Phys. Rev.* **B37**, 2792 (1988)
- [19] O K Andersen, *Phys. Rev.* **B12**, 3060 (1975)
- [20] M Methfessel and S Frota-Pessôa, *J. Phys.: Condens. Matter* **2**, 149 (1990)
- [21] A R Williams, J Kübler and C D Gelatt Jr, *Phys. Rev.* **B19**, 6094 (1979)
- [22] H Eschrig, *Optimized LCAO Method and the Electronic Structure of Extended Systems* (Springer, Berlin, 1989)
- [23] B Meyer, K Hummler, C Elsässer and M Fähnle, *J. Phys.: Condens. Matter* **7**, 9201 (1995)
- [24] A Dalgarno, *Proc. R. Soc. (London)* **A251**, 282 (1959)
- [25] E Paschalis and Al Weiss, *Theor. Chim. Acta.* **13**, 381 (1967)
- [26] L Pauling, *The Nature of Chemical Bond*, 3rd edn (Cornel University Press, Ithaca, NY, 1960)
- [27] K J Duff and T P Das, *Phys. Rev.* **168**, 43 (1968)